ELSEVIER

Chemical Engineering Journal 80 (2000) 167–175

Chemical Engineering Journal

www.elsevier.com/locate/cej

Hydrodynamic parameters from the Michaels and Bolger method

R. Font [a,*], M. Pérez [b,1]

[a] *Departamento de Ingeniería Química, Universidad de Alicante, Apartado Correus 99, 03080 Alicante, Spain*
[b] *Departamento de Ingeniería de Sistemas y Comunicaciones, Universidad de Alicante, Apartado 99, 03080 Alicante, Spain*

Abstract

For different initial heights and solids concentration of flocculated calcium carbonate suspensions in the compression range, the variations of the subsidence rates are discussed in accordance with the Michaels and Bolger method. A mathematical model based on the consolidation theory has been applied to generalize the Michaels and Bolger method, and to discuss the relationships between the permeability, the effective pressure and the solids concentration. In accordance with this model and the experimental results, it is deduced that the relationship between the effective pressure and the solids concentration differs considerably from that obtained by other methods, whereas the values of permeability for different solids concentration are close to those deduced by different methods. © 2000 Elsevier Science B.V. All rights reserved.

Keywords: Sedimentation; Compression; Permeability; Michaels and Bolger method

1. Introduction

This paper discusses the sedimentation batch test with calcium carbonate suspensions in the compression range, when the suspension can be considered a network of channels through which the fluid flows upwards, while the solids are flowing downwards. The behavior of flocculated suspensions can be characterized by the relationships between the effective pressure of solids, the permeability and the solids concentration. In the compression range, the sedimentation of the solids takes place as a consequence of the unbuoyed weight of the upper solids minus the friction force exerted by the liquid flowing upwards between the solids as considered and stated by different authors: Michaels and Bolger [1], Shirato et al. [2], Smiles [3], Blake and Colombera [4] and Kos [5]. It is assumed that the solids structure responds instantaneously to stress change as discussed by Fitch [6,7], Tiller [8] and Font [9] and so the volume fraction of solids. ε_s is a function of the effective pressure p_s. Bustos and Concha consider the variation of momentum with respect to time in a one-dimensional conservation equation [10].

Shirato et al. [2], Fitch [6], Tiller [8] and Font [9] used the Darcy equation to analyze batch sedimentation as indicated in the following equation:

$$-\frac{\partial p_s}{\partial x} = (\rho_s - \rho)\, g\, (1-\varepsilon) + \frac{\partial p^+}{\partial x} = (\rho_s - \rho)\, g\, (1-\varepsilon) - (\mu\varepsilon/k)\,(u - u_s) \quad (1)$$

where p^+ is the manometric, dynamic or hydraulic excess liquid pressure.

The effective pressure p_s on each layer of particles is the result of the downward force of the unbuoyed weight of aggregates minus the upward force of friction due to Darcian flow. The values ε and ε_s are the volume fraction of voids or porosity, and the volume fraction of solids in the sediment, respectively, u and u_s the average velocity of liquid and settling solids respectively, μ is the liquid viscosity and k is the permeability. The velocities are considered positive when the direction is upwards. For batch testing sedimentation where u and u_s have opposite signs, it can be written that:

$$u\varepsilon + u_s\,(1-\varepsilon) = 0 \quad (2)$$

and from Eq. (2), it is possible to deduce that:

$$u - u_s = -u_s/\varepsilon \quad (3)$$

Considering Eqs. (2) and (3), Eq. (1) becomes [6,8,9]

$$-\frac{\partial p_s}{\partial x} = (\rho_s - \rho)\, g\varepsilon_s - (\mu/\mathrm{k})\,(-u_s) \quad (4)$$

Eq. (4) can be employed to explain the basis of the Michaels and Bolger model [6].

Michaels and Bolger assumed that at the initial moment, only the pulp at the bottom of the vessel is compressing, thus integrating Eq. (4) between $x = 0$ (bottom of the vessel)

* Corresponding author. Tel.: +34-6-5903546; fax: +34-6-5903826.
E-mail addresses: rafael.font@ua.es (R. Font), manolo@disc.ua.es (M. Pérez).
[1] Tel.: +34-6-5903400; fax: +34-6-5903682.

1383-5866/00/$ – see front matter
PII: S1383-5866(00)00088-5

Nomenclature

C_1	$((k\varepsilon_s{}^3)/\mu)(dp_s/d\varepsilon_s)$; consolidation coefficient variable throughout the column and time (m^2/s)
C_2	$-((g\Delta\rho\omega_o\varepsilon_s{}^2)/\mu)d(k\varepsilon_s)/d\varepsilon_s$; modified consolidation coefficient variable throughout the column and the time (m^2/s)
D_o	diameter of the container tube (m)
D_y	yield diameter (m)
e	local void of the suspension equals $\varepsilon/(1-\varepsilon)$
$f(t)$	permeability factor varying with time
f_k	parameter in Eq. (40)
f_p	pressure factor of Eq. (41)
g	gravity acceleration (m/s^2)
H	height of the pulp-supernatant interface (m)
h	dimensionless height of each interval throughout the column $h=1/(n+1)$
H_y	parameter of Eq. (9) (m)
H_o	initial height of the suspension at $t=0$ (m)
H_m	height corresponding to the bottom of the constant zone (m)
k	permeability coefficient (m^2)
K_1	$k(\varepsilon_s)\varepsilon_s/\mu$; modified permeability coefficient (m^4/N s)
n	interval numbers of the column
p^+	manometric, dynamic or hydraulic excess pressure (N/m^2)
p_s	effective pressure of solids (N/m^2)
p_{sm}	maximum pressure of solids at the bottom of the vessel (N/m^2)
t	time (s)
t_m	parameter in Eq. (40) (s)
u	fluid velocity (m/s)
u_s	solid sedimentation velocity (m/s)
u'_s	settling velocity of solids in absence of compressive force (m/s)
x	distance down column (m)
$y_i{}^j$	value of dimensionless pressure $\Phi(z, t)$ at interval i and time j
z	ω/ω_o; dimensionless coordinate used in the simulation process ($0 \le z \le 1$)

Greek letters

$\varphi_i{}^j$	function given by Eq. (39)
$\varepsilon = 1-\varepsilon_s$	porosity or fraction of liquid in suspension (m^3 liquid/m^3 suspension)
ε_s	volume fraction of solids (m^3 solid/m^3 suspension)
ε_{so}	initial volume fraction of solids in suspension (m^3 solid/m^3 suspension)
τ	interval of time (s)
$\Phi(z, t)$	$p_s(z, t)/\Delta\rho g\omega_o$; dimensionless solid pressure
Φ_m	maximum dimensionless solid pressure at the bottom of the column (N/m^2)
μ	viscosity of liquid (Kg/ms)
ρ	density of liquid (kg/m^3)
ρ_s	density of solids (kg/m^3)
ω	volume of solids per unit area at distance x to the bottom (m)
ω_o	initial value of ω: $\omega_o=\varepsilon_{so}H_o$; total volume of solids per unit of area
υ	rising rate of the non constant concentration zone above the bottom

and $x=H_o$ (initial height of suspension) where the solids pressure is nil, it can be written that:

$$-\int_{p_{sm}}^{0} dp_s = \int_0^{H_o} g(\rho_s-\rho)\varepsilon_s dx - \int_0^{H_o} (\mu/k(\varepsilon_s))(-u_s)\,dx \quad (5)$$

$$p_{sm} = g(\rho_s-\rho)\varepsilon_{so}H_o - (\mu/k(\varepsilon_{so}))(-u_{so})H_o \quad (6)$$

where p_{sm} is the solids pressure at the bottom of the column at $t=0$, ε_{so} is the initial fraction volume of solids, $k(\varepsilon_{so})$ is the suspension permeability value at $\varepsilon_s=\varepsilon_{so}$, and $(-u_{so})$ is the initial batch settling rate of the pulp in the compression range.

Introducing the settling velocity of solids $(-u'_s)$ in the absence of compressive force (i.e. when H_o is infinite) and the height H_y, defined as the height of solids that can be sustained by a solids pressure equal to p_{sm} at the bottom of vessel where $(-u_s)$ is zero, it can be deduced from Eq. (6) that

$$g(\rho_s-\rho)\varepsilon_{so} = (\mu/k(\varepsilon_{so}))\left(-u'_s\right) \quad (7)$$

$$p_{sm} = g(\rho_s-\rho)\varepsilon_{so}H_y \quad (8)$$

and substituting Eqs. (7) and (8) in Eq. (6), the Michaels and Bolger relationship is obtained:

$$(-u_s) = \left(-u'_s\right)\left(1-\left(H_y/H_o\right)\right) \quad (9)$$

Note that in the previous equations, the wall effects have been considered negligible. Considering the wall effects, Eq. (9) should be written as

$$(-u_s) = \left(-u'_s\right)\left(1-\left(H_y/H_o\right)-\left(D_y/D_o\right)\right) \quad (10)$$

where D_o is the diameter of the container tube and D_y is the yield diameter [1].

The parameters H_y and $(-u'_s)$ can be determined as follows. For a given initial concentration of the fraction volume of solids ε_{so} and several tests with different values of H_o, the corresponding values of $(-u_{so})$ are obtained. A plot of $(-u_s)$ versus $1/H_o$ should be a straight line in accordance with Eq. (9). The intercepts with the $1/H_o$ and $(-u_s)$ axes

give the parameters H_y and $(-u'_s)$ respectively. It can be observed that from these values, the constitutive relationships

$$p_s = p_s(\varepsilon_s) \quad (11)$$

$$k = k(\varepsilon_s) \quad (12)$$

can be obtained for different initial solids concentration through Eqs. (7) and (8).

It is curious that Fitch [6,11] proposed the use of the relationships obtained by the Michaels and Bolger method to obtain the relationship between the permeability and the maximum settling velocity $(-u'_s)$ when there is no solids stress gradient, whereas the relation between the effective pressure and the solids concentration is obtained by another method (considering the average solids concentration of different sludges with different heights at time infinity when there is no subsidence rate in any layer).

On the other hand, Font et al. [12] showed with experimental data of calcium carbonate suspensions, that the values of permeability obtained by the Michaels and Bolger method were similar to those obtained considering data of solids concentration at the sediment of a batch test, whereas the relationship $p_s = f(\varepsilon_s)$ obtained from the Michaels and Bolger method is very different from that obtained considering the average solids concentration with different sediment heights at time infinity.

Relationships (11) and (12) are useful for the design of thickeners, simulation and for characterization of the suspension [11,13–16].

Michaels and Bolger [1] used kaolin suspensions with low values of the volume fraction of solids in the 0.0023–0.0065 range, and probably in the non-compression range, the method seems incorrect. The aim of this paper is to analyze the method proposed by the Michaels and Bolger model, for determining the relationships between the effective pressure of solids, the permeability and the solids concentration.

2. Materials

Commercial calcium carbonate was used to prepare the suspensions. The chemical composition was the following: $CaCO_3 = 98.47$ wt.%; $MgCO_3 = 1.00$ wt.%; $Fe_2O_3 = 0.016$ wt.%; $SiO_2 = 0.22$ wt.%; $Al_2O_3 = 0.20$ wt.%. The average surface particle diameter obtained by laser diffraction and X-ray absorption sedimentation techniques was 3.6 μm. The granulometric weight distribution was the following: <2 μm 10%, between 2 and 4.6 μm 20%, between 4.6 and 7.6 μm 20%, between 7.6 and 12 μm 20%, between 12 and 22 μm 20%, and between 22 and 80 μm 10%. All experiments presented in this paper correspond to suspensions with similar hydrodynamic behavior. The experiments were carried out at 20°C in graduated cylinders at different heights, from 0.6 to 1.2 m and with an internal diameter equal to 0.06 m. The particle density at 20°C was 2554 kg/m^3. The wall effects were considered negligible.

3. Experimental results

The experimental results were obtained from 23 batch tests with different initial solids concentration at the compression range and with different initial heights. Five series with initial volume fractions of solids 0.152, 0.187, 0.197, 0.200 and 0.216 were carried out, with initial heights between 1.1 and 0.5 m. Experiments at greater values of solids concentration were not considered because the discontinuity did not descend at horizontal level. Fig. 1 shows the results of a series corresponding to different initial heights and the same initial volume fraction of solids.

It can be observed that the slopes (absolute values) of the settling curves initially increase with time, then become nearly constant and after a period of the time decrease continuously. The increasing slope of the settling curve at the beginning of the tests is probably due to the fact that the structure of the aggregates network changes with time and with channeling formation, as occurs in the sediment in batch testing with the initial solids concentration in the non-compression range [16]. Nevertheless this aspect is discussed later. The values of $(-u_s)$ are obtained from the slope corresponding to the straight line drawn after the induction period (Fig. 1).

In order to determine the values of parameters H_y and $(-u'_s)$ for a given concentration, values of $(-u_s)$ versus $1/H_o$ are plotted, as shown in Fig. 2. The intercepts of the straight lines with the $1/H_o$ axis give the values of $1/H_y$, and the intercepts with the $(-u_s)$ axis give the $(-u'_s)$ values. Table 1 shows the values obtained of p_{sm} and the permeability k, considering the experimental data shown in Fig. 2, in accordance with Eqs. (7)–(9).

The values of the permeability were determined in the range of ε_s between 0.152 and 0.216 and, as indicated in a previous paper [12], agree with those obtained by other methods, considering batch tests with determination of the solids concentration at different heights and times [12]. The value of the critical or gel volume fraction of solids was 0.152. The permeability values can be satisfactorily correlated with the volume fraction of solids ε_s by the

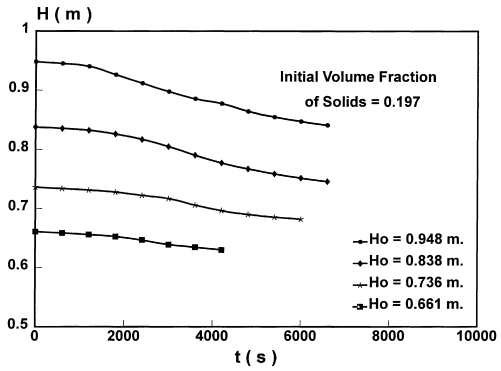

Fig. 1. Batch tests in accordance with the Michaels and Bolger method.

Table 1
Values of permeability and solids pressure

ε_s (m^3 sol./m^3 sus.)	$(-u'_s)\times10^5$ (m/s)	$1/H_y$ (m^{-1})	$k\times10^{11}$ (m^2)	p_{sm} (N/m^2)
0.152	7.43	3.56	3.12	650
0.187	5.58	2.33	1.96	1222
0.197	5.18	2.04	1.72	1470
0.200	4.94	1.95	1.61	1561
0.216	3.87	1.78	1.17	1848

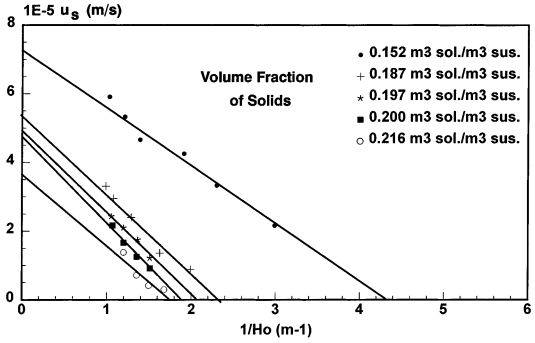

Fig. 2. Settling rates vs. the inverse of initial height in accordance with the Michaels and Bolger method.

equation

$$k = \exp\left[-19.63\varepsilon_s^3 - 51.66\varepsilon_s^2 + 5.09\varepsilon_s - 23.54\right] \quad (m^2) \tag{13}$$

for $0.152 \leq \varepsilon_s \leq 0.216$.

The values of p_{sm} as a function of solids concentration, obtained by the Michaels and Bolger method are adjusted to the following potential law:

$$p_s = 2.031 \cdot 10^5 \cdot \varepsilon_s^{3.0447} \quad (N/m^2) \tag{14}$$

for $0.152 \leq \varepsilon_s \leq 0.216$.

The values of p_s deduced from Eq. (13) are much greater than the values obtained from the sediment height at time infinity [12], correlated by the following equation:

$$p_s = 61.752 \cdot \ln(0.3199/(0.4755 - \varepsilon_s)) \quad (N/m^2) \tag{15}$$

For the values of ε_s between 0.152 and 0.216, the values of p_s deduced from Eq. (13) are 150–200 times the values obtained from Eq. (14). This great discrepancy could be due to a change of the structure, and is discussed in this paper. In addition, it can be deduced that the value of p_s for the critical or gel solids concentration ($\varepsilon_s = 0.152$–0.155) is nil in accordance with Eq. (15) whereas a value around 550 N/m^2 is obtained using Eq. (14).

4. Batch test simulation in the compression range

In order to discuss whether the Michaels Bolger method may be applied, a mathematical model taking into account the principles of soil mechanics is considered. The mathematical model is based on the consolidation theory, originally developed by Terzaghi and Peck [17], and also used later by Shirato et al. [2,18]. This model explains the settling of slurries due to the consolidation and electroforced sedimentation in the compression range.

The principles of the consolidation theory are applicable to the analysis of settling with compactation or compression, i.e. when the initial volume fraction of solids is larger than the so-called critical value or gel concentration ε_{s1} ($\varepsilon_{s1} = 0.155$ for calcium carbonate used in this paper [12]). Nevertheless, some important differences can be noted between the consolidation theory and the settling of slurries in the compression range.

In the consolidation theory, the consolidation coefficients remain constant (in accordance with Terzaghi's theory). However, this assumption is not applicable to compressible sediments, and the analytical or computerized solutions must be obtained for variable consolidation coefficients. The basic equations of the model are expressed as a function of the material coordinate ω, defined as

$$\omega = \int_0^x \varepsilon_s \mathrm{d}x \tag{16}$$

where ω is the volume of solids per cross-sectional area between the bottom and the layer at distance x as can be seen in Fig. 3.

Introducing the material coordinate (Shirato et al. [2,18]), the equations of continuity and momentum conservation can be written as

$$\frac{\partial(-u_s)}{\partial\omega} = -\frac{\partial e}{\partial t} \tag{17}$$

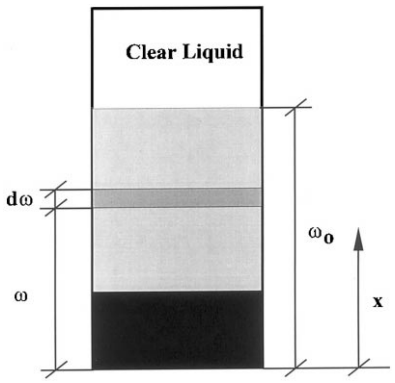

Fig. 3. Definition of material coordinates used in simulation.

$$-\varepsilon_s \frac{\partial p_s}{\partial \omega} = g(\rho_s - \rho)\varepsilon_s - \frac{\mu}{k(\varepsilon_s)}(-u_s) \quad (18)$$

where e is the void ratio of the suspension defined as

$$e = \varepsilon/(1-\varepsilon) = (1-\varepsilon_s)/\varepsilon_s \quad (19)$$

Differentiating Eq. (18) with respect to ω and substituting $\partial(-u_s)/\partial\omega$ into Eq. (17), it can be deduced that

$$-\frac{\partial e}{\partial t} = \frac{\partial K_1}{\partial \omega}\left[g(\rho_s - \rho) + \frac{\partial p_s}{\partial \omega}\right] + K_1 \frac{\partial^2 p_s}{\partial \omega^2} \quad (20)$$

where K_1 is the modified permeability coefficient defined as

$$K_1 = k(\varepsilon_s)\varepsilon_s/\mu \quad (21)$$

Assuming that the void ratio e is only a function of the solid compressive pressure p_s, it is deduced that

$$e = e(p_s) \quad (22)$$

$$\frac{\partial e}{\partial t} = \frac{\partial p_s}{\partial t}\left(\frac{\mathrm{d}p_s}{\mathrm{d}e}\right)^{-1} \quad (23)$$

Substituting Eq. (23) into Eq. (20) and rearranging yields

$$\frac{\partial p_s}{\partial t} = -K_1 \frac{\mathrm{d}p_s}{\mathrm{d}e}\frac{\partial^2 p_s}{\partial \omega^2} - \frac{\mathrm{d}K_1}{\mathrm{d}e}\left[\left(\frac{\partial p_s}{\partial \omega}\right)^2 + (\rho_s - \rho)\left(\frac{\partial p_s}{\partial \omega}\right)\right] \quad (24)$$

Introducing the following notation

$$\left.\begin{aligned} C_1 &= -K_1 \frac{\mathrm{d}p_s}{\mathrm{d}\varepsilon_s}\frac{\mathrm{d}\varepsilon_s}{\mathrm{d}e} = \frac{k(\varepsilon_s)\varepsilon_s^3}{\mu}\frac{\mathrm{d}p_s}{\mathrm{d}\varepsilon_s} \\ C_2 &= \omega_o g(\rho_s - \rho)\frac{\mathrm{d}K_1}{\mathrm{d}\varepsilon_s}\frac{\mathrm{d}\varepsilon_s}{\mathrm{d}e} \\ &= -\left(\frac{g(\rho_s - \rho)\omega_o \varepsilon_s^2}{\mu}\right)\frac{\mathrm{d}[k(\varepsilon_s)\varepsilon_s]}{\mathrm{d}\varepsilon_s} \end{aligned}\right\} \quad (25)$$

and considering the dimensionless coordinates

$$\Phi = p_s/(g(\rho_s - \rho)\omega_o) \quad z = \omega/\omega_o \quad (26)$$

Eq. (24) yields the mathematical model of the batch sedimentation with compression expressed in dimensionless coordinates:

$$\frac{\partial \Phi(z,t)}{\partial t} = \left(\frac{C_1(z,t)}{\omega_o^2}\right)\frac{\partial^2 \Phi(z,t)}{\partial z^2} - \left(\frac{C_2(z,t)}{\omega_o^2}\right) \times \left[\left(\frac{\partial \Phi(z,t)}{\partial z}\right)^2 + \frac{\partial \Phi(z,t)}{\partial z}\right] \quad (27)$$

Eq. (27) is a non-linear partial differential equation of the parabolic type.

Equations similar to Eq. (27) but with other coordinate systems are considered by Shirato et al. [2,18], Kos [5], Smiles [3] and Blake and Colombera [4]. The constitutive equations relating k and p_s with the volume fraction of solids ε_s, must be known for integrating Eq. (27).

Eq. (27) cannot be integrated analytically and must therefore be solved numerically, together with Eqs. (13) and (14) or Eq. (15) considering the boundary and initial conditions. The boundary conditions are the following:

(i) For $z = 1$ (top of the sediment where the material coordinate ω is constant and equals ω_o the solids pressure is always nil, so

$$(\Phi)_{z=1} = 0 \quad (28)$$

(ii) For $z = 0$ (bottom of the vessel where $\omega = 0$) the sedimentation velocity is zero and from the momentum conservation equation (Eq. (18)), it is deduced that

$$-\varepsilon_s \frac{\partial p_s}{\partial \omega} = g(\rho_s - \rho)\varepsilon_s \Rightarrow \left(\frac{\partial \Phi}{\partial z}\right)_{z=0} = -1 \quad (29)$$

In order to define an initial condition $\Phi(z, 0)$, the Michaels and Bolger model [1] can be considered. At the initial moment $t = 0$, the suspension concentration remains constant throughout the column. The permeability and the sedimentation velocity are therefore also constant, so Eq. (6) can be written in material coordinate as

$$\varepsilon_{so} p_{sm} = g(\rho_s - \rho)\varepsilon_{so}\omega_o - (\mu/k(\varepsilon_{so}))(-u_{so})\omega_o \quad (30)$$

Integrating Eq. (18) between $\omega = 0$ and an arbitrary value ω, where the solids pressure is p_s, leads to

$$\varepsilon_{so}(p_{sm} - p_s) = g(\rho_s - \rho)\varepsilon_{so}\omega - (\mu/k(\varepsilon_{so}))(-u_{so})\omega \quad (31)$$

Eliminating $(\mu/k(\varepsilon_{so}))(-u_{so})$ between Eqs. (30) and (31), the solids pressure in dimensionless coordinates (Eq. (26)) can be expressed as

$$\Phi(z, 0) = \Phi_m(1 - z) \quad (32)$$

where Φ_m is the maximum value of dimensionless pressure at the bottom of vessel

$$\Phi_m = p_{sm}/(g(\rho_s - \rho)\omega_o) \quad (33)$$

In accordance with Eq. (33), the solids pressure at the initial moment varies linearly from zero at the top of the sediment to a maximum value p_{sm} at the bottom of the vessel. Fig. 4 shows the initial distribution of solids pressure as a function of the dimensionless coordinate z, and a possible distribution after a time $t_1 > 0$. It is possible to know the value of $(p_{sm})_{t=t_1}$ from Eq. (14), which was determined at the time $t > 0$ in accordance with the Michaels and Bolger model.

For integrating Eq. (27), an explicit difference scheme of three layers was used, that has been explained extensively in another paper [19]. This scheme is unconditionally stable and has no restriction in the integration step. It is therefore possible to carry out the integration very quickly in comparison with other methods. A forward difference approximation is used for the partial derivative with respect to time, so it can be written that

$$\frac{\partial \Phi(z,t)}{\partial t} \approx \frac{y_i^{j+1} - y_i^j}{\tau} \quad (34)$$

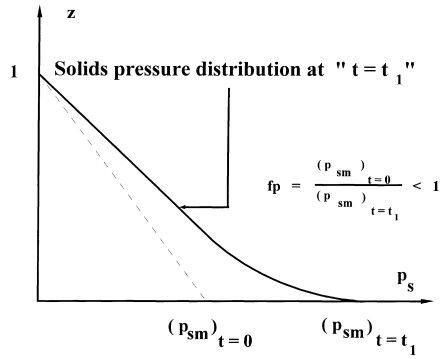

Fig. 4. Distribution of solids pressure at times $t=0$ and $t=t_1$.

where the superscript $j+1$ denotes the values at time $t+\Delta t$ and j refers to those values at time t, and the spatial location is given by subindex i. A central difference approximation is employed for the first and second derivatives with respect to z, so it is possible to obtain the approximation at time t and distance z as follows:

$$\left.\begin{aligned}\frac{\partial \Phi\,(z,t)}{\partial z} &\approx \frac{y_{i+1}^{j}-y_{i-1}^{j}}{2h}\\ \frac{\partial^2 \Phi\,(z,t)}{\partial z^2} &\approx \frac{y_{i+1}^{j}-\left(y_i^{j+1}+y_i^{j-1}\right)+y_{i-1}^{j}}{h^2}\end{aligned}\right\} \tag{35}$$

where h equals $1/(n+1)$ and $n+1$ is the number of spatial intervals (see Fig. 5).

Taking into account Eqs. (27)–(29), Eq. (3) and Eq. (35), the following equations are deduced:

$$\left.\begin{aligned}&\frac{y_i^{j+1}-y_i^{j-1}}{2.\tau}=\frac{(C_1)_i^{j}}{\omega_0^2}\cdot\\ &\times\left[\frac{y_{i+1}^{j}-(y_i^{j+1}+y_i^{j-1})+y_{i-1}^{j}}{h^2}\right]+\varphi_i^{j}\\ &i=1,2\ldots\quad;\quad 1\le i\le(n+1)\end{aligned}\right\} \tag{36}$$

$$y_i^0=\frac{p_{\mathrm{sm}}}{g\,(\rho_{\mathrm{s}}-\rho)\,\omega_{\mathrm{o}}}\left(1-\frac{i-1}{n}\right) \tag{37}$$

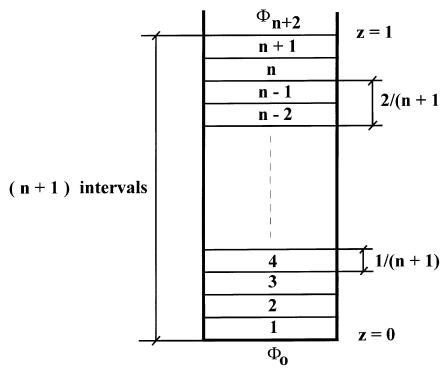

Fig. 5. Intervals throughout the column expressed in material coordinates.

$$y_{n+1}^{j}=0\quad;\quad\frac{y_2^{j}-y_0^{j}}{2h}=-1 \tag{38}$$

where the function φ_i^{j} is defined as

$$\varphi_i^{j}=-\frac{(C_2)_i^{j}}{\omega_{\mathrm{o}}}\left[\left(\frac{y_{i+1}^{j}-y_{i-1}^{j}}{2h}\right)^2+\frac{y_{i+1}^{j}-y_{i-1}^{j}}{2h}\right] \tag{39}$$

In Eq. (39), the domain of y has been extended one step to the other side of the boundary, considering an imaginary point y_0^{j} that is eliminated from the boundary derivative condition.

The difference scheme of three layers has a disadvantage in that it is not self-starting, since the values of the solution are needed at both y_{o} and y_1 before the method can be applied for the first time. This problem is overcome with a difference scheme of two layers which gives the starting values necessary to carry out the integration process.

5. Results and discussion from the simulation

In order to discuss the Michaels and Bolger method for obtaining the constitutive relationships (Eqs. (11) and (12)), several simulations have been carried out with the mathematical model developed in this work. The simulation program was prepared using Matlab, calculating the distribution of the concentration and the pressure of solids, and the sedimentation velocity throughout the column at different times.

In all cases, Eq. (27) was integrated with the boundary and initial conditions explained previously. In each case, the constitutive relationships $k=f(\varepsilon_{\mathrm{s}})$ and $p_{\mathrm{s}}=f(\varepsilon_{\mathrm{s}})$ are different.

5.1. Case I: the relationships $k=f(\varepsilon_s)$, $p_s=f(\varepsilon_s)$ are those obtained directly by Eqs. (13) and (15)

In this case, the relation $k=f(\varepsilon_{\mathrm{s}})$ used is that deduced from the Michaels and Bolger method, with no correction factor. The relation $p_{\mathrm{s}}=f(\varepsilon_{\mathrm{s}})$ used is Eq. (15), obtained from the sediment heights at time infinite [12]. Fig. 6 shows the variation of the supernatant suspension height versus time and also the experimental values. It can be observed that there is a great discrepancy between the experimental results and the simulated ones, obtained with Eqs. (13) and (15).

5.2. Case II: the relationships $k=f(\varepsilon_s)$, $p_s=f(\varepsilon_s)$

$$\left.\begin{aligned}k(\varepsilon_{\mathrm{s}},t)&=f(t)\cdot\exp[-19.63\varepsilon_{\mathrm{s}}^3-51.66\varepsilon_{\mathrm{s}}^2\\ &\quad+5.09\varepsilon_{\mathrm{s}}-23.54]\\ f(t)&=\frac{1}{f_k-\dfrac{(f_k-1)t}{t_m}}\ \text{ for }\ t\le t_{\mathrm{m}}\\ f(t)&=1\ \text{ for }\ t>t_{\mathrm{m}}\end{aligned}\right\} \tag{40}$$

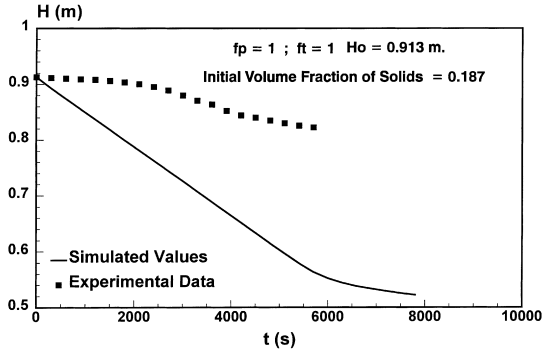

Fig. 6. Experimental values of the pulp-supernatant interface and values obtained by simulation in case I. Parameters: $\varepsilon_{so} = 0.187$, $H_o = 0.913$ m, $f_p = 1$, $f(t)$=1.

and

$$p_s = f_p \cdot 2.031 \cdot 10^5 \cdot \varepsilon_s^{3.0447} \quad (41)$$

In the constitutive relationships (Eqs. (40) and (41)), the permeability and the solids pressure deduced from the Michaels and Bolger method, are used with correction factors, indicated in the index of Fig. 7, as follows:

1. For the permeability, a correction factor $f(t)$ is included (Eq. (40)), so the permeability is a function of the time and the factor $f(t)$ for $t = 0$ equals $1/f_k$ and the permeability is f_k times lower than the value obtained from Eq. (13). When $t = t_m$, $f(t)$ equals 1, the permeability does not depend on the time. This is due to the fact that the suspension is less permeable at the beginning of the test than later when the channels are formed.
2. For the effective pressure, another factor f_p is also considered, because the relationship $p_s = f(\varepsilon_s)$ deduced from the Michaels and Bolger method is obtained from the straight line H–t after an initial induced period of time (see Fig. 4).

Fig. 7 shows the experimental and simulated variation of the supernatant suspension interface for three runs, where the values of f_k, t_m and f_p have been considered. It can be seen that there is a good correlation of the experimental data with the simulation program, with the boundary and initial conditions and with the correction factors. For the other tests, good correlations were also obtained, but with their corresponding values of f_k, t_m and f_p close to those of the experiments shown in Fig. 7.

The value of factor f_p is considered in accordance with the following fact. It was deduced that the solids pressure at $t = 0$ is a straight line from the Michaels and Bolger model. However, the solids pressures p_{sm} are obtained at $t > 0$, considering the initial height H_o, instead of another height less than H_o, because the zone of constant concentration has decreased (this will be considered in Fig. 10). Therefore for evaluating $(p_{sm})_{t=0}$, it is necessary to introduce the factor $f_p < 1$ that multiplies $(p_{sm})_{t>0}$. This factor is unknown and must be introduced in the simulation program to adjust the simulation values to the experimental one. Values of 0.6–0.8 have been used to obtain a good agreement between the simulated and experimental results.

If any of the correction expression are not used, the experimental results cannot be simulated correctly. Using other expressions for the correction factor, the experimental data can also be correlated. The relationship $p_s = f(\varepsilon_s)$ can also change with the time, because the final sludge height is less than that predicted experimentally. Nevertheless, a variation of $p_s = f(\varepsilon_s)$ with time has not been considered, because this is not necessary for the purpose of this paper.

5.3. Case III: the relationships $k = f(\varepsilon_s)$, $p_s = f(\varepsilon_s)$

$$k(\varepsilon_s) = \exp\left[-19.63\varepsilon_s^3 - 51.66\varepsilon_s^2 + 5.09\varepsilon_s - 23.54\right] \quad (42)$$

$$p_s = f_p \cdot 2.031 \cdot 10^5 \varepsilon_s^{3.0447} \quad (43)$$

In this case, there is no correction factor changing with time for the permeability. Fig. 8 shows the simulated results together with the experimental points. It can be observed that there is no induction period of increasing settling rate with the simulated data.

It can be also deduced that, in this hypothetical case, considering the absence of permeability changing with time, there is a considerable decrease in the settling rate along the

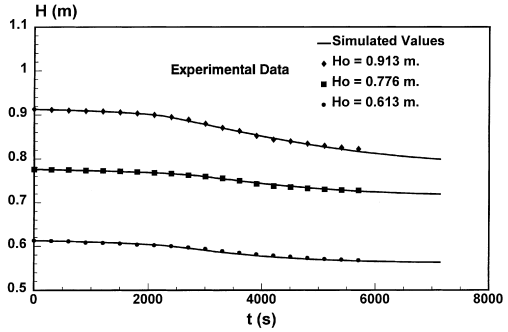

Fig. 7. Experimental and simulated values of the upper interface obtained in case II. Parameters: $\varepsilon_{so} = 0.187$, Run ◇ $f_p = 0.60$, $f_k = 13$, $t_m = 3000$ s.; Run □ $f_p = 0.76$, $f_k = 12.7$, $t_m = 3000$ s; Run ○ $f_p = 0.59$, $f_k = 8$, $t_m = 2400$ s.

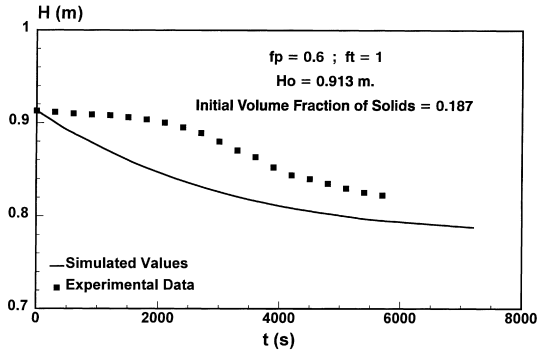

Fig. 8. Experimental and simulated values of the upper interface obtained in Case III. Parameters: $\varepsilon_{so} = 0.187$, $H_o = 0.913$ m, $f_p = 0.60$, $f(t) = 1$.

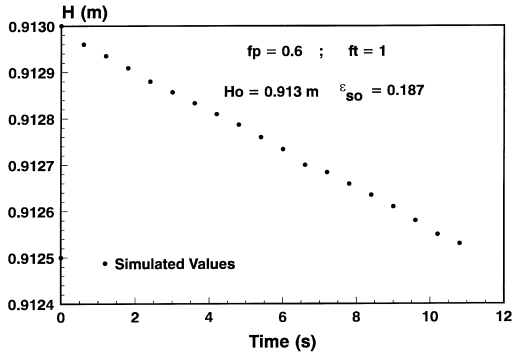

Fig. 9. Upper discontinuity during the first period of time obtained in Case III. Parameters: $\varepsilon_{so}=0.187$, $H_o=0.913$ m, $f_p=0.6$, $f(t)=1$.

run. There is another interesting aspect in the simulation of this case.

Fig. 9 shows the variation of the upper discontinuity during a short period of time (case III). Note that the value of $(-u_s)$ obtained by the program is equal to that observed during the first few seconds. If other values are considered, the program produces numerical instabilities.

Fig. 10 shows the variation of the upper discontinuity and the zone of constant concentration with time for the case III. It can be observed that whereas the upper discontinuity descends very slowly, the zone of concentration greater than ε_{so} rises very quickly. An explanation of this fact is discussed as follows: At any time, considering the balance of forces applied to the zone of constant concentration it can be written that

$$p_{sm}=(g\,(\rho_s-\rho)\,\varepsilon_{so}-(\mu/k\,(\varepsilon_{so}))\,(-u_s))\,(H-H_m) \quad (44)$$

where p_{sm} and $k(\varepsilon_{so})$ are the solids pressure and permeability corresponds to the initial solids concentration ε_{so}, H is the height of the pulp-supernatant interface, and H_m is the height corresponding to the bottom of the zone of constant concentration. Note that Eq. (44) leads to Eq. (8) at the beginning of the test when $H=H_o$ and $H_m=0$. On the other hand, the rising velocity of the layer of constant concentration can be written as:

$$\upsilon=\frac{dx}{dt}=-\frac{\partial\varepsilon_s/\partial t}{\partial\varepsilon_s/\partial x} \quad (45)$$

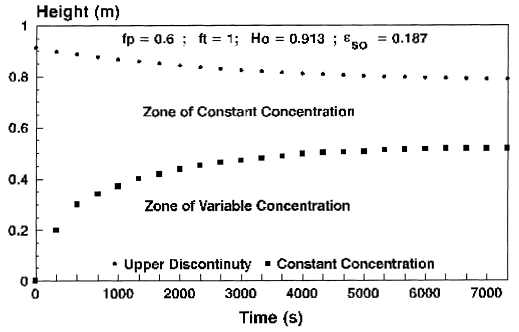

Fig. 10. Variation of the upper discontinuity and the region of constant concentration. Parameters: $\varepsilon_{so}=0.187$, $H_o=0.913$ m, $f_p=0.6$, $f(t)=1$.

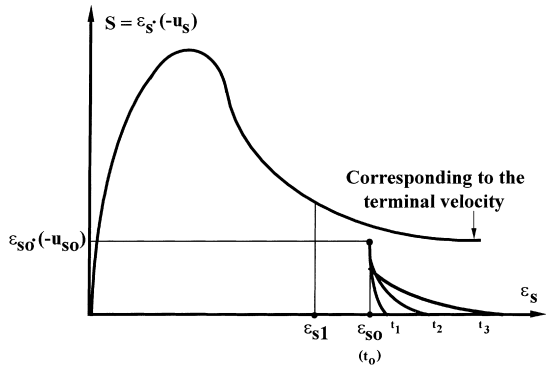

Fig. 11. Flux density vs. volume fraction of solids.

and considering the continuity equation

$$\frac{\partial\varepsilon_s}{\partial t}-\frac{\partial\,[\varepsilon_s\,(-u_s)]}{\partial x}=0 \quad (46)$$

it can be deduced that

$$\upsilon=-\frac{\partial\,[\varepsilon_s\,(-u_s)]\,/\partial x}{\partial\varepsilon_s/\partial x}=-\frac{\partial\,[\varepsilon_s\,(-u_s)]}{\partial\varepsilon_s} \quad (47)$$

where υ changes with time.

Considering the flux diagram $(-u_s)\varepsilon_s$ versus ε_s shown in Fig. 11, the initial consolidation considered corresponds to all the suspension with constant concentration ε_{so} and subsidence rate of $(-u_{so})$, and the layer at the bottom with constant concentration ε_{so} and $(-u_{so})$ equals zero. After an initial period of time, the variation of the flux of the solids can be similar to that indicated in Fig. 11, so the rising velocity υ corresponding to the layer of height H_m is very great. Consequently, if the variation of H_m is great, in accordance with Eq. (44) the variation of $(-u_s)$ must also be great, as shown with the simulation program (Fig. 9). This means, that although the Michaels and Bolger hypothesis can be considered as correct at $t=0$, the observed velocity, after an initial period of time, without effects of changing permeability, would be less.

In practice, the permeability also changes with time and the initial settling rate is determined experimentally after an initial period, in which there is also a considerable change in the height of the zone of constant solids concentration and, consequently, this does not exactly correspond to the initial conditions.

In spite of these aspects, the variation of $k=f(\varepsilon_s)$ agrees with that obtained by other methods. This is probably due to the fact that at great initial heights, the settling rate is close to the maximum possible. On the other hand, the relationship $p_s=f(\varepsilon_s)$ obtained from the Michaels and Bolger method is not representative of the consolidation process, due to two reasons: (a) values of pressure are necessary to force the formation of channels, and (b) the application of the Michaels and Bolger method is only approximate as shown previously.

The simulation results show that there is a region extending from the upper interface downwards, whose volume fraction of solids is constant and equal to the concentration of the original suspension at time $t = 0$. This zone decreases with time until it disappears when the suspension reaches the equilibrium state at $t = \infty$. This fact is proved from data obtained by means of X-rays [20,21] and similar to those obtained by simulation in this paper, in accordance with the Michaels and Bolger model [1].

An extension of the paper could be the consideration of the inertial effects on the momentum balance as taken into account by Bustos and Concha [10]. Fig. 6 shows the variation of the experimental height and simulated height of the supernatant–suspension interface versus time. The simulated variation was obtained considering the relationships between the permeability, the effective solids pressure and the solids concentration corresponding when channels are formed and the solids settle faster than when channels are not formed. The shape of the experimental variation cannot be justified considering single inertial effects of acceleration or deceleration, so these inertial effects although than can be important probably cannot explain the experimental variation.

6. Conclusions

The Michaels and Bolger method for determining the constitutive relationship between the permeability and the solids concentration of a suspension in a compression range, must be considered as an approximate method, due to the following reasons:

1. The Michaels and Bolger method is based on the tangents to the curve *H–t*, obtained in batch testing with initial concentration of solids in the compression range, after an initial period. Under this condition, the settling process is advanced, and the zone of constant solids concentration equal to the initial one has discussed when channeling is fully developed.
2. The results of the simulation show that the constitutive relationships (Eqs. (11) and (12)) must change with time, and both the solids pressure and permeability obtained by Eqs. (7) and (8) are different to the initial conditions. This means that the extrapolation by the Michaels and Bolger method must be considered as approximate. It has also been tested that the Michaels and Bolger method is not useful for determining the constitutive relationship $p_s = p_s(\varepsilon_s)$, due to the fact that solids pressures are necessary to form channels through which liquid circulates upwards, greater than those corresponding when channels are formed.

References

[1] A.S. Michaels, J.C. Bolger, Ind. Eng. Chem. Fundam. 1 (1962) 24.
[2] M. Shirato, T. Aragaki, A. Manabe, AIChE J. 25 (1979) .
[3] D.E. Smiles, Chem. Eng. Sci. 31 (1976) 273.
[4] J.R. Blake, P.M. Colombera, Chem. Eng. Sci. 32 (1977) 221.
[5] P. Kos, Gravity Thickening of Sludges, Ph.D. thesis, University of Massachusetts, Amherst, 1977.
[6] B. Fitch, AIChE J. 25 (1979) 913.
[7] B. Fitch, AIChE J. 29 (1983) 940.
[8] F.M. Tiller, AIChE J. 27 (1981) 823.
[9] R. Font, AIChE J. 34 (1988) 229.
[10] M.C. Bustos, F. Concha, AIChE J. 34 (1988) 859.
[11] B. Fitch, Ing. Eng. Chem. 58 (1966) 18.
[12] R. Font, M. Pérez, C. Pastor, Ind. Eng. Chem. 33 (1994) 2859.
[13] D.C. Dixon, Chem. Eng. Sci. 36 (1981) 499.
[14] K.A. Landman, L.R. White, R. Buscall, AIChE J. 34 (1988) 239.
[15] F.M. Tiller, W. Chen, Chem Eng. Sci 43 (1988) 1695.
[16] R. Font, Chem. Eng. Sci. 46 (1991) 2473.
[17] K. Terzaghi, R.B. Peck, Soil Mechanics in Engineering Practice, Wiley, New York, 1948.
[18] M. Shirato, H. Kato, K. Kobayasi, H. Skazaki, J. Chem. Eng. Jpn. 3 (1970) 98.
[19] M. Pérez, R. Font, C. Pastor, Comp. Chem. Eng. 22 (1998) 1531.
[20] M. Gaudin, M.C. Fuersteneau, Preprint, Intern. Mining Proc. Congr. London, April, 1960.
[21] F.M. Tiller, Catscan analysis of sedimentation and constant pressure filtration, in: Proceedings of the Fifth World Filtration Congress, Nice, 1991.